Development and comparison of different injury risk functions predicting pelvic fractures in side impact for a Human Body Model

J. Peres, S. Auer, N. Praxl

Abstract Human Body Models (HBMs) provide increased biofidelity and additional measurement capabilities compared to dummies. However, at present injury prediction is mostly limited to binary assessments based on physical thresholds and therefore doesn't allow for a population-based probabilistic estimation. In this study, different Injury Risk Curves (IRCs) predicting pelvic fractures were developed for the Total Human Model for safety (THUMS) v4.02 AM50. These IRCs are based on two types of metrics, namely global metrics and local metrics. Global metrics are based on force measurements whereas local metrics are based on strains. A large set of post-mortem human subject (PMHS) experimental tests was reproduced with the THUMS v4, then the different metrics were measured and correlated to the injuries observed in the experiments. Different indicators were used to assess and compare the fracture prediction capabilities of the different IRCs.

Keywords Pelvic fracture, Injury Risk Curve, THUMS, Side impact, Human body models.

I. INTRODUCTION

Around 30% of all car occupant crash-related deaths are the result of side impact [1]. Protection of the occupant in side impact remains a challenge, despite the improvements in occupant protection provided by the introduction of side and curtain airbags and strengthening of the vehicle structure. The pelvis is the second most AIS2+ injured body region in side impact [2], with significant societal costs [3]. The most common AIS2+ injuries to the pelvis are in this order: pubic ramus, acetabular and illium fractures [4-5].

Numerical models of the human body represent a promising tool for safety engineers. The evolution from lumped mass models [6] to today´s million elements Finite Element (FE) Models has resulted in significant improvements. Parallel to the extension of their application in the Industry and in the research community, their quality and validity have also increased dramatically. Toyota Motor Corporation and Toyota Central R&D Labs are developing the THUMS family in this regard. The most detailed model of the THUMS family is the version 4 [7], which was first released in 2010. The Global Human Body Model Consortium (GHBMC) is an international initiative regrouping industrial and academic partners to continually develop the GHBM family, which includes highly detailed and biofidelic HBMs [8]. The THUMS v4 and the GHBM are to date state of the art FE Models of the human body.

Despite the previously described improvements, injury prediction is largely limited to threshold-based criterion leading to a binary assessment. Some efforts are being made to allow the personalization of the models [9-10], potentially allowing injury assessment for any specific individual. However, the amount of biomechanical variability makes it necessary to introduce a statistical approach in order to assess the risk for a greater portion of the population using a reduced set of models. Despite the extended use of injury risk curves (IRCs) for ATDs, few have been proposed for HBMs. Forman *et al*. [11] proposed an IRC to predict rib fractures for a modified version of the THUMS v3 model. The IRC was built based on rib coupon tests reported by Kemper *et al*. [12] and used peak strain, including age adjustment, as a predictor of rib fracture. However, when using probabilistic criterion, it appears that direct translation of dummy criterion to HBMs is still the most common approach. Load path through the pelvis was studied by Salzar *et al*. [13] and by Leport *et al*. [14]. The latter performed non-injurious impactor and mini-sled tests on eight PMHS instrumented with pubic loadcells. Leport *et al*. identified the ratio between the external impactor force on the pelvis and the pubic force. This ratio was

J. Peres (e-mail: Jeremie.peres@pdb-org.com; tel: +49 (0)84 189-43683) and N. Praxl are Research Engineers at the Partnership for Dummy Technology and Biomechanics (PDB). S. Auer is a Bachelor degree student at OTH Regensburg.

used to calculate the pubic force for 90 PMHS tests reported in the literature and ultimately an IRC based on the pubic force was proposed. In 2012, on behalf of the ISO/TC22/SC12/WG6, Petitjean *et al*. [15] developed IRCs for the WSID dummy. The pubic force was used as injury criteria for pelvis injuries and AIS2+ and AIS3+ IRCs were developed.

In the current paper we intend to develop IRCs predicting AIS2+ pelvic injuries for the THUMS v4.02-AM50 in side impact. A set of lateral impact tests from the literature was selected and simulated, and the results were used to develop IRCs using various injury predictors.

II. METHODS

Normalizing

Datasets of biomechanical tests commonly contain PMHS with characteristics (e.g. height, mass, bone/soft tissue behavior, etc.) different from an average male. It is therefore not correct to correlate directly the injury outcome of these PMHS to the response of a 50th percentile surrogate, whether it is a dummy or a HBM. Normalizing techniques have been developed to enable the use of PMHS tests performed with PMHS of different sizes than the surrogate [16-17]. Two approaches have been proposed: in the first, the boundary conditions (impactor mass or velocity) are normalized in order to expose the surrogate to a severity level equivalent to a given PMHS; in the second, the results obtained with the surrogate are normalized to the PMHS anthropometry. These scaling techniques are based on mass-spring models and a set of assumptions, such as geometric similarity. In this study we decided to scale the velocity of the impactor in the simulations according to the following equation [18]:

$$V_{50th} = V_{xxth} * \sqrt{\frac{m_{50th} + m_{imp}}{m_{xxth} + m_{imp}}} \qquad (1)$$

where V_{50th} and m_{50th} are the impact speed and the mass for the 50th surrogate, V_{xxth} and m_{xxth} are the impact speed and the mass for the PMHS, and m_{imp} is the mass of the impactor.

In order to investigate the validity of the assumptions inherent to these scaling techniques, we used two HBMs, one having the geometry of a 50th (GHBM-M50-O v4.4) and the other the geometry of a 95th male (GHBM-M95-O v1-1). A set of tests was selected and simulated with both models. Two simulations were performed with the 95th HBM, one with the nominal impactor velocity and the other with a velocity scaled according to Equation 1. The correlations between the strains observed in the pelvis cortical bone of the 50th HBM and the 95th model with scaled and unscaled velocities permitted a conclusion on the benefit of the normalization to achieve an equivalent severity level. The list of the configurations tested and corresponding velocities are given in Table I, while description of the test series can be found in the following section. The mass of the GHBM-M50 and GHBM-M95 are 76.8 kg and 103.3kg, respectively.

TABLE I
TEST SELECTION FOR SCALING CHECK

Test series	Impactor mass (kg)	Nominal velocity (m/s)	Scaled velocity (m/s)
Leport impactor	23.4	3.7	4.0
Leport mini-sled	91.0	3.5	3.6
Cesari	17.3	5.8	6.3
Cesari	17.3	10.9	11.9
Cesari	17.3	14.8	16.2
Bouquet 1994	23.4	3.4	3.6
Bouquet 1994	23.4	6.8	7.3
Bouquet 1998	16	7.0	7.7
Bouquet 1998	16	11.5	12.6
Bouquet 1998	12	13.7	15.2

Guidelines were defined by the expert of the ISO/TC22/SC12/WG6 [18] for the development of IRCs. These guidelines were followed step-by-step and are detailed later in this paper. The first step consisted of collecting the relevant PMHS data, and it is described in the following section.

Test selection

Tests reported in the literature were analyzed and only dynamic tests involving seated, full body PMHS loaded only or partially on the pelvis in lateral impacts were included in the database. Data of tests with multiple impacts where weakening of the specimen had been detected as described by ISO [18] were excluded, as well as tests involving a padded impactor surface. The test series used for the development of the IRCs are summarised below.

Cesari et al.

ONSER performed two series of impactor tests on the pelvis of PMHS seated on a low friction surface [19-20]. The greater trochanter was impacted by means of a 17.3 kg rigid impactor, the surface of which was a portion of a sphere (R=60 mm, r=175 mm). The velocity was increased until fracture was observed.

Marcus et al.

Marcus *et al.* [21] reported a series of tests using the Heidelberg sled configuration. The wall consisted of separated plates for the thorax and the pelvis and impact velocities varied from 6.4 m/s to 11.3 m/s.

Zhu et al.

In 1993 Wayne State University (WSU) described cadaver tests using a five plates sled (shoulder, thorax, abdomen, pelvis, knee) [22]. Impact velocities ranged from 6.4 m/s to 11.3 m/s.

Pintar et al. and Kuppa et al.

Pintar *et al.* in 1997 [23] and Kuppa *et al.* in 2003 [24] reported tests using the National Highway Traffic Safety Administration (NHTSA) wall and velocities from 6.7 m/s to 8.9 m/s. The wall consisted of four plates for the thorax, the abdomen, the pelvis and the lower extremities. Different configurations were tested, including plate offsets.

Bouquet et al. 1994

In this test series [25], cadavers were seated on a low friction surface and impacted by a 23.4 kg, 200*100 mm plate centered on the greater trochanter. Each cadaver was hit first at a lower/non-injurious velocity (approximately 3.5 m/s) and then at a higher velocity (approximately 6.7 m/s).

Bouquet et al. 1998

Later, Bouquet *et al.* [26] performed similar tests but with a larger (200*200 mm) and lighter (12 kg and 16 kg) impactor, but at higher impact velocities (9.9 m/s to 13.7 m/s).

Leport et al.

Leport *et al*. [14] reported non-injurious tests performed at CEESAR in 2007 using two types of configuration, namely mini-sled and impactor. Impactor mass was 23.4 kg and the impacting surface was a portion of a sphere, as reported in Cesari *et al*., and velocities ranged from 3.5 m/s to 5.1 m/s. The mini-sled surface was 200*350 mm with a mass of 91 kg and impacted the pelvis at velocities from 3.3 m/s to 4.0 m/s.

Petit et al.

PMHS and WSID tests were performed at CEESAR and reported in 2015 [27]. Nine tests were performed in three configurations, which were designed to maximize the risk of sacro-iliac joint (SIJ) rupture. In all three series the impactors had a mass of about 150 kg and rigid surfaces that were not parallel to the sagittal plane. Impact speeds for configuration 1, 2 and 3 were 8.0 m/s, 5.4 m/s and 7.5 m/s, respectively. This test series will be referred in this paper as SI Joint.

A summary of the simulated tests can be found in Table VI. In total, 106 tests were reconstructed corresponding to 95 PMHS. Eleven cadavers were tested twice in the same test series, once at non-injurious

energy level and subsequently at an injurious energy level. Out of the 106 simulated tests, 41 resulted in AIS2+ injuries.

Modeling of the selected tests

Depending on the test series, the initial position of the PMHS in the tests was not always comprehensively described. Therefore, it was decided to use a standard position for the model in all the simulated configurations. This position is the most commonly reported in the experimental tests (see Figs 1 and 2) and was obtained by way of pre-simulation. The arms are positioned so that the hands lie just over the thigh, and the pelvis reference plane is positioned with an angle of 45° relative to the horizontal. Lower limbs were symmetrical and parallel to each other, leading to a distance of approximately 250 mm between the middle of both knees. Lower legs were located at an angle of 45° relative to the upper legs. The model was seated on a rigid surface using pre-simulation leading to a slight compression of the buttock and thigh tissues.

All simulations were performed using LSDyna MPP version 6.11 r.78769. Bone failure was deactivated to allow measurement of maximum strain. The contact between impacting surface and the HBM was defined using the option *AUTOMATIC_SURFACE_TO_SURFACE, including edge-to-edge treatment, and contact thickness was standardized to 1 mm for all simulations. The contact between the seat and the HBM used a low coefficient of friction of 0.1 to reproduce low friction surfaces reported in all test series. In all sled tests, the model was given an initial velocity towards the wall, whereas in impactor tests or mini sled tests the initial velocity was assigned to the impactor. The impact velocity was personalized for each PMHS test according to Equation 1; initial velocities for each simulation can be found in Table VI.

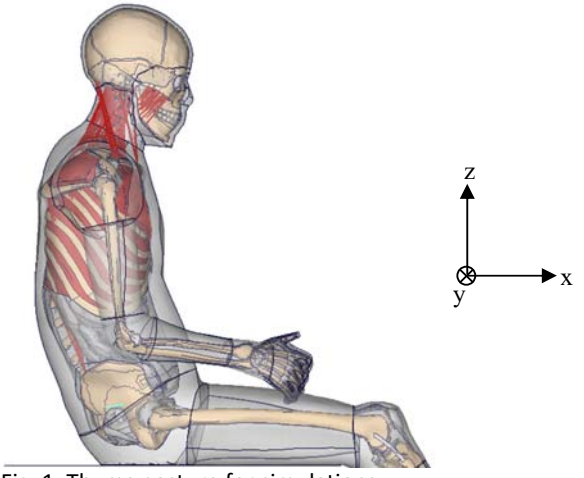

Fig. 1. Thums posture for simulations.

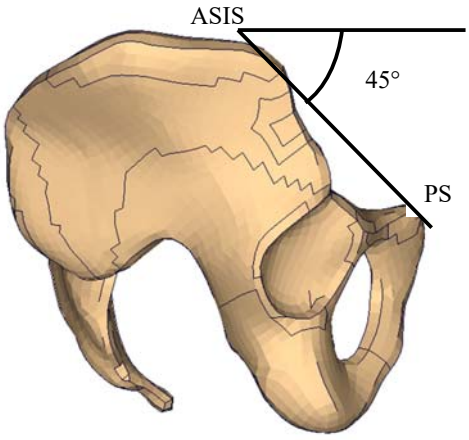

Fig. 2. Thums pelvis orientation.

Several assumptions were made in the simulations due to some parameters of the PMHS tests not being explicitly known. For example if the position of the PMHS is in most cased at least roughly described, it could have varied slightly between the different experiments. The orientations of the pelvis, the arms and the legs were not always reported and most likely not always measured. Friction coefficients with the impactors and with the seat were not known but assumed to be low. What´s more to ease the simulation process, the model was pre-seated and we did not use a gravity set which would likely lead to more realistic interactions. To estimate the potential influence of those assumptions on the results, we performed a parametric study varying the posture of the THUMS model, the friction coefficients and seating the model in the seat using gravity. Posture variations are illustrated in Figs 3-5. The friction coefficient was increased from 0.1 initially to 0.3 and the gravity set consisted in applying gravity to the THUMS model until the reaction force of the seat reached an equilibrium and, in the same run, simulating the impact immediately after. The parameter study was performed using the setup from Pintar *et al.* and Kuppa *et al.* as it involved a wall impacting the whole body leading to potential influence of the arms posture. Results were compared to a reference simulation using the standard position and friction parameters.

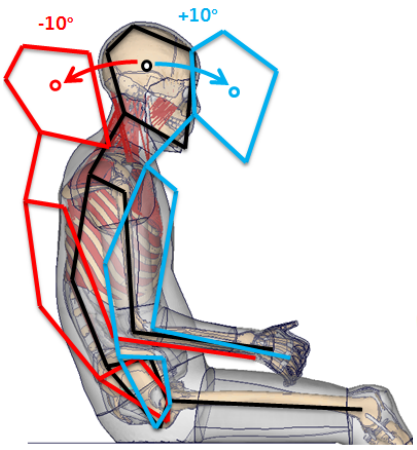

Fig. 3. Rotation of the pelvis +-10° in the y direction.

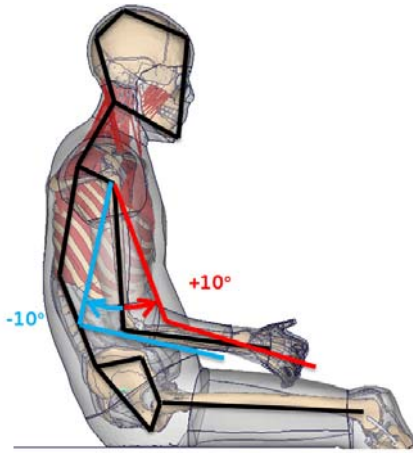

Fig. 4. Rotation of the upper arm +-10° in the y direction.

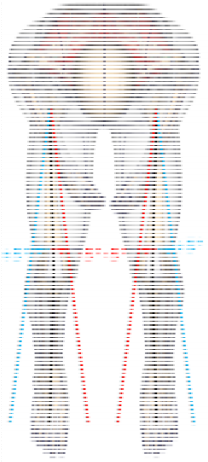

Fig. 5. Rotation of the legs +-10° in the z direction.

Description of the Injury Predictors

Different injury predictors were tested, and these predictors can be split in two categories: force-based and strain-based. Three force-based predictors were investigated in this study:

1. -The impactor force, which in the case of the sled test was measured on the pelvic plate.
2. -The pubic force, which is the injury criteria used for the WSID dummy. It was measured using a cross- section at the pubic symphysis (PS) level and only the y component was used.
3. -The sum of the pubic and the SIJ force, which represents the total force transmitted to the pelvic bone. The SIJ force was measured in the ilium, close to the joint.

Three strain predictors were tested, all based on the Maximum Principal Strain (MPS), and these strains were measured on the cortical bone elements of the whole pelvis, including the sacrum. For each element the maximum MPS over the whole duration of the simulation was recorded and the MPS distribution over the whole pelvis was generated, as illustrated in Fig. 6. Based on this distribution, the 100th, 99th and 95th percentile were calculated and used as injury predictors, later referred as MPS, MPS99 and MPS95.

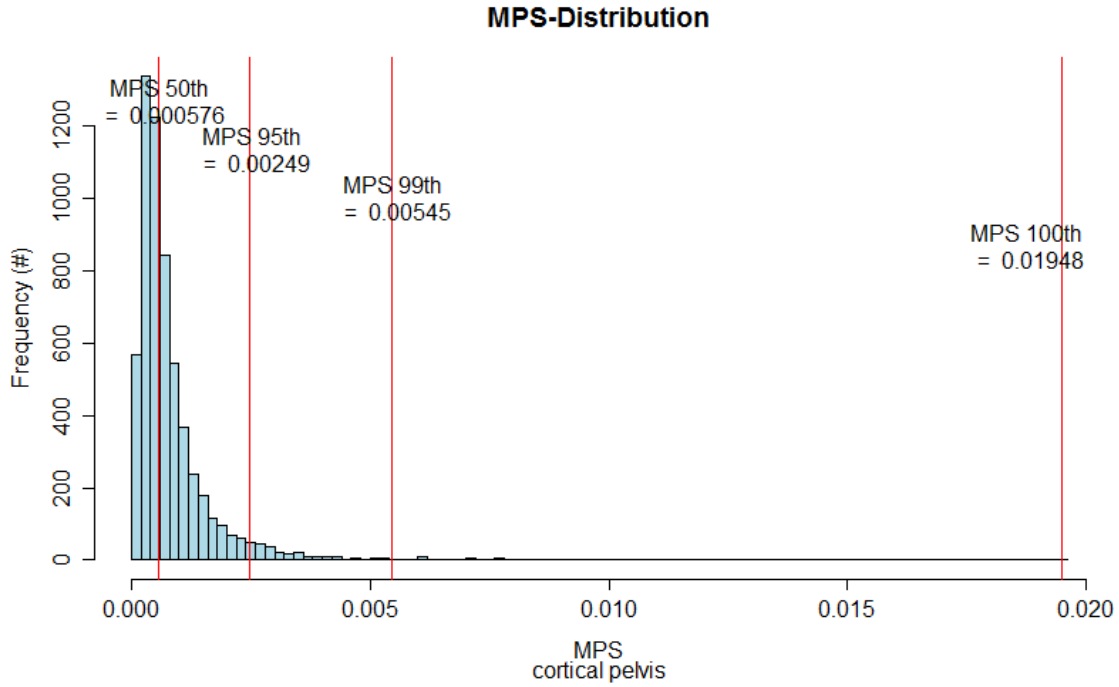

Fig. 6. Example of an MPS distribution.

Development of the IRCs

As described above, the ISO/TC22/SC12/WG6 guidelines were followed, which consist of 11 steps to develop the IRC. The maximum likelihood method was used to estimate the parameters of three different probability distributions, namely the Weibull, log-normal and log-logistic, taking into account the censoring of the data by utilising the survival analysis method implemented in the statistical software R. The three resulting parameterised distributions without age adjustment were compared to the non-parametric maximum likelihood estimate (NPMLE) to assess their validity. QQ plots, the Akaike Information Criteria (AIC) for both age-adjusted and non-adjusted distributions, as well as the Receiver Operating Characteristic (ROC) and associated area under the curve (AUC), were used to further assess the quality of each predictor and associated distributions. The 95% confidence intervals of the IRCs were also calculated and quality index of the IRC was determined for 5%, 25% and 50% risks of injury according to the guidelines of ISO/TC22/SC12/WG6. Finally, for the best injury predictors, IRCs are proposed for 45 and 65 years old.

III. RESULTS

Validation of the normalizing method

The strains (MPS, MPS99 and MPS95) obtained with GHBM M95 with a scaled and an unscaled impactor velocity are plotted against the strains obtained with the GHBM50 on Figs 7, 8 and 9. For all three strain metrics, the scaling improved the correlation between the 50th and 95th percentile models.

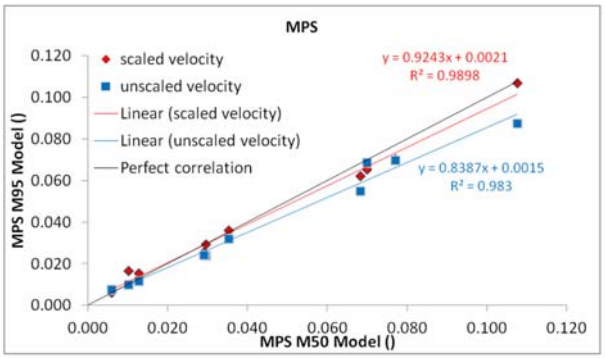

Fig. 7. MPS correlation between M50 and M95 with and without velocity scaling.

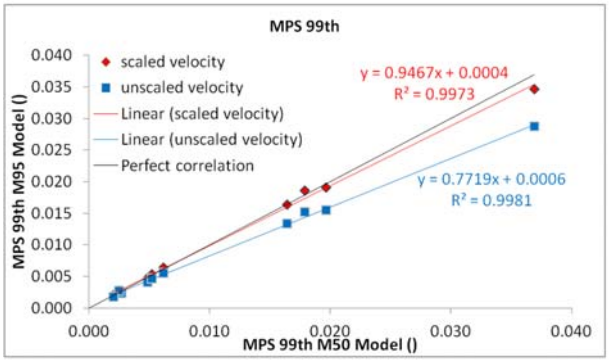

Fig. 8. MPS99 correlation between M50 and M95 with and without velocity scaling.

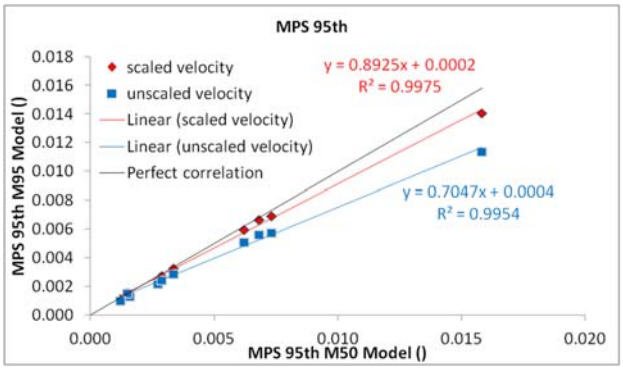

Fig. 9. MPS95 correlation between M50 and M95 with and without velocity scaling.

Set-up validation

In order to validate the modeling assumptions for the simulated load cases, the pelvis impactor force measured in a representative set of experimental tests and in the corresponding simulations were compared. PMHS tests were selected if the mass of the cadaver was close to the mass of the THUMS model and the cadaver preferably did not sustain any injury. Results obtained for this set are presented in Table II. If the impact surface consisted of more than one plate, only the force measured on the pelvic plate was compared. For the SI Joint series, there

was not always a cadaver having a weight comparable to the 50th percentile, therefore all experimental tests are reported.

TABLE II
RESULTS OF SET-UP VALIDATION

Test series	Test ref.	PMHS ref.	AIS	PMHS mass (kg)	Impact speed (m/s)	Exp. Pelvic imp. force (N)	Sim. Pelvic imp. force (N)
Cesari	C2	C	0	78	8.83	10120	9494
Marcus	H-82012	H-82012	0	75	11.31	30474	30394
Leport mini-sled	PCH1770	571	0	77	3.5	4770	4264
Leport Impactor	IMP563	583	0	77	3.8	3610	3308
Kuppa	SC111	NA	0	76	6.7	14413	13286
Zhu	SIC07	SIC07	0	74.8	6.7	6680	10489
Bouquet 1994	MRB03	MRT02	0	76	3.4	6220	3211
SI Joint Config. 1	PCH2123	MS663	4	60	8.0	12200	
	PCH2124	MS664	3	62.5	8.1	11300	15957
	PCH2125	MS665	0	95	7.9	14500	
SI Joint Config. 2	PCH2128	MS666	2	55	5.4	5100	
	PCH2129	MS667	2	69	5.4	6300	5678
	PCH2130	MS668	2	78.5	5.4	9300	
SI Joint Config. 3	PCH2132	MS669	0	64	7.5	15100	15692
	PCH2134	MS671	0	107	7.5	13500	

Generally, the forces obtained in the simulations correlate well with the experiments, however for Bouquet 1994 the force measured in the experiment (6220 N) is almost twice as big as the force measured in the simulation (3211 N). MRB03 was the test for which the measured impactor force was the highest despite some cadaver being heavier than MRT02. Ten tests were run at 3.346+-0.09 m/s and resulted in an average Force of 4341+-1013 N. Subsequently, the 10 PMHS were hit at a higher velocity, and four of these tests at higher energy did not result in injuries. Among those non-injured tests, the average Force was 9150+-1746 N and the average velocity was 6.55+-0.09 m/s. The corresponding simulation with THUMS v4 AM50 led to a pelvic force of 7666 N.

The pelvic force in SIC07 is much higher in the simulation than in the experiment, however the test SIC05 performed in the same condition led to a Force (normalized to a 50th male) of 10670 N, which is close to the simulation force (10489 N). Overall, the forces measured in the simulations correlate well with the forces reported for the experiments, therefore all test series were retained for the development of the IRCs.

Parametric study

TABLE III
RESULTS OF THE PARAMETRIC STUDY

Variant	Impact Force (N)	Pubic Force (N)	PS+SIJ Force (N)	MPS without acet. ()	MPS with acet. ()	MPS99 without acet. ()	MPS99 with acet. ()	MPS95 without acet ()	MPS95 with acet. ()
Standard	14900	2998	6743	0.0270	0.0270	0.0073	0.0088	0.0047	0.0049
Arm-10°	16432	3084	6696	0.0255	0.0255	0.0065	0.0083	0.0044	0.0046
Arm+10°	15055	3146	6506	0.0253	0.0253	0.0072	0.0092	0.0047	0.0050
Legs-5°	17195	3098	6870	0.0253	0.0253	0.0075	0.0101	0.0048	0.0052
Legs+5°	14209	3019	6658	0.0218	0.0218	0.0072	0.0088	0.0047	0.0050
Pelvis-10°	16092	2944	6570	0.0221	0.0221	0.0069	0.0080	0.0044	0.0047
Pelvis+10°	14379	3308	6675	0.0287	0.0287	0.0075	0.0089	0.0046	0.0050
Friction0.3	14700	3032	6835	0.0260	0.0260	0.0072	0.0086	0.0046	0.0049
Gravity	15008	3061	6775	0.0212	0.0212	0.0068	0.0078	0.0045	0.0047
Max deviation	0.015	0.103	0.035	0.215	0.215	0.110	0.148	0.064	0.061

The values of all predictors obtained for the test SAC109 with the standard configuration and with the previously described parameter variations are presented in table III. In the last line of that table, we specified the maximum percentage of deviation from the standard simulation for all predictors. The sum of the pubic and SIJ forces is very steady over all variations (only 3.5% maximum deviation) meaning that the overall force transmitted to the pelvis bone structure is almost constant. MPS with or without acetabulum exhibit the most deviations (21.5%). Considering a lower percentile of the MPS distribution leads to lower deviation in the results, MPS95 being the most robust strain predictor.

Simulation results

Table VI details the results of all the simulations run with the THUMS v4 AM50. High strains were systematically observed at the acetabulum in the THUMS model, including in configurations where no acetabulum fractures were reported in the experiments. It is believed that the modeling of the hip joint in the THUMS, the femur head contacting the acetabulum directly and not through cartilaginous tissues, could lead to a systematic overestimation of the strains in the acetabulum. In an attempt to reduce the influence of this modeling limitation in the IRCs, strains were post-treated twice for each simulation, once including and once excluding the acetabulum elements from the strain distribution. Figures 10 and 11 show the injured and non-injured tests as a function of age and MPS95 including and excluding the acetabulum. The same trend is observed for all predictors, showing increasing injury occurrence with increasing age and severity.

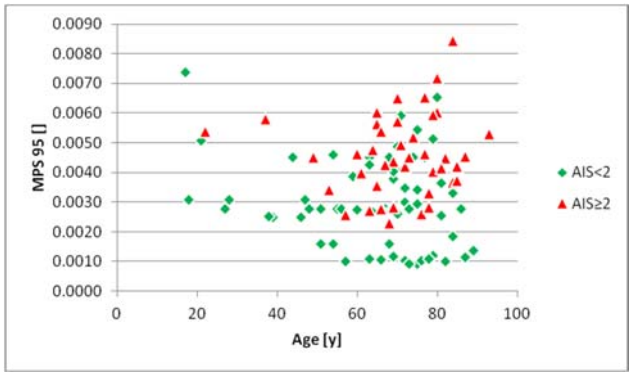

Fig. 10. Injury outcome as a function of MPS95 and age for all simulated tests when including acetabulum.

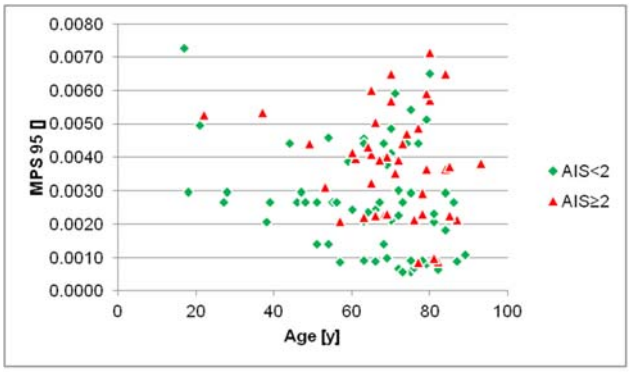

Fig. 11. Injury outcome as a function of MPS95 and age for all simulated tests when excluding acetabulum.

Injury risk curves

Figures 12–14 show QQ plot, comparison of fitted distribution to NPMLE and IRC, including 95% confidence intervals for the impactor force with a Weibull distribution without age adjustment for the average PMHS age. Figures 15–17 show the same metrics for MPS95 and a log-normal distribution. The log-normal distribution for MPS95 seems to match the NPMLE more closely than the Weibull distribution for impactor force, nonetheless both acceptably follow the non-parametrical estimate. Overall, all predictors and parametric distributions seem to lead to reasonable match of the NPMLE and rather narrow 95th confidence intervals. Generally, confidence intervals were narrow for low severity levels but getting wider for higher severities. Best distributions were for all global predictors Weibull and for all local predictors log-normal, the log-logistic distribution systematically resulting in higher AIC values.

An attempt was made to adjust the distribution using the mass of the PMHS as an additional parameter as it was hypothesized that the mass could correlate to the bone quality and ultimately to the mechanical tolerance of the cadavers. This attempt did not lead to significant improvements in the evaluation metrics and it was thus decided not to use mass as an adjustment parameter.

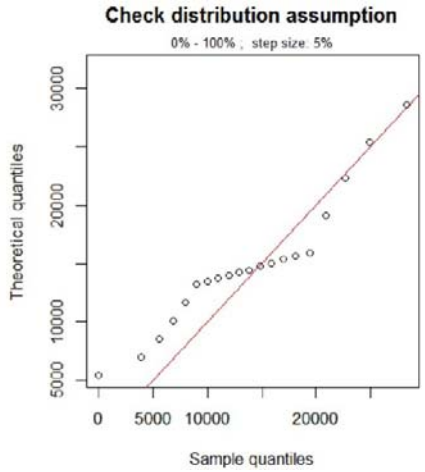

Fig. 12. QQ plot for impactor Force Weibull fit.

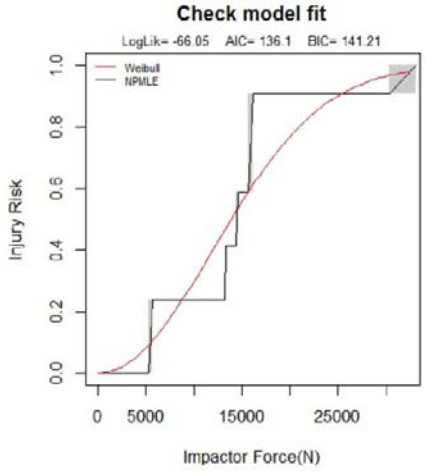

Fig. 13. NPMLE for impactor Force vs Weibull fit.

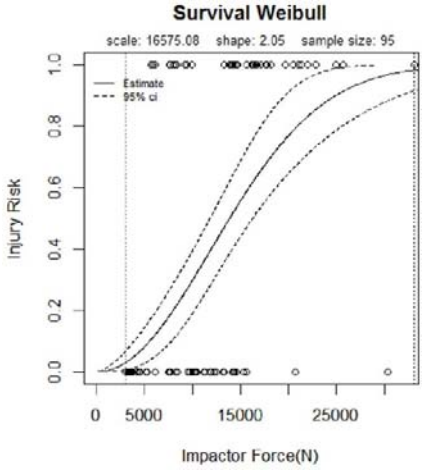

Fig. 14. IRC without age adjustment for impactor Force Weibull fit.

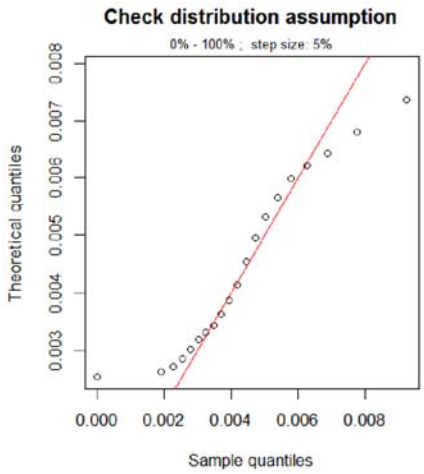

Fig. 15. QQ plot for MPS95 Normal fit.

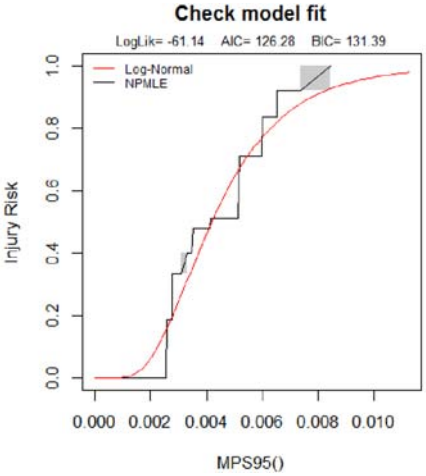

Fig. 16. NPMLE for MPS95 vs Normal fit.

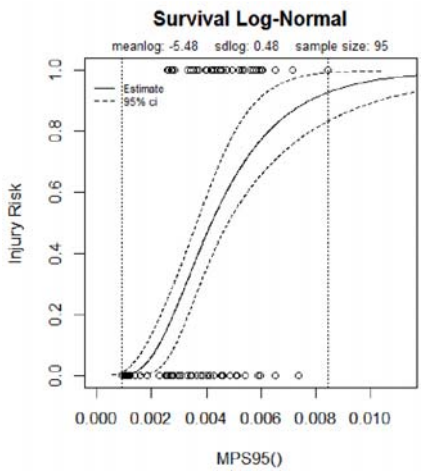

Fig. 17. IRC without age adjustment for MPS95 Normal fit.

Table IV outlines values of the metrics used for evaluating the IRCs for all predictors and the distribution that led to the lowest age-adjusted AIC. Quality indexes and AUC are given for the IRC with age adjustment.

TABLE IV
EVALUATION OF THE BEST DISTRIBUTIONS FOR EACH PREDICTOR

Predictor	Distribution	AIC		QI at 5%	QI at 25%	QI at 50%	AUC
		Without age	With age				
Impactor Force	Weibull	136.1	125.5	0.32	0.17	0.13	0.77
Pubic Force	Weibull	150.4	142.9	0.34	0.17	0.13	0.71
PS+SI	Weibull	143.8	135.9	0.26	0.14	0.12	0.72
MPS without acet.	Log-normal	125.4	121.2	0.30	0.18	0.16	0.81
MPS with acet.	Log-normal	123.9	125.4	0.26	0.16	0.14	0.80
MPS99 without acet.	Log-normal	128.8	130.0	0.29	0.18	0.17	0.79
MPS 99 with acet.	Log-normal	125.9	123.5	0.24	0.14	0.12	0.80
MPS 95 without acet.	Log-normal	134.9	130.3	0.27	0.19	0.18	0.78
MPS 95 with acet.	Log-normal	126.3	122.6	0.26	0.13	0.12	0.80

IV. DISCUSSION

The results obtained for the impactor force are surprisingly good in comparison with other predictors, particularly when comparing to the pubic force. Indeed, it was proven that the transmission of the load through the pelvis bone depends strongly on the shape and area of the impactor [13-14]. It is especially believed that there is a significant difference between the impacts involving only the greater trochanter and those involving iliac wing only or both greater trochanter and iliac wing, which would advocate against impactor force. It could be that PS force can only predict accurately pubic rami fractures and is unable to detect injury mechanisms for which the main load does not go through the pubis. However, about three-quarters of injuries to the pelvis reported in side impacts are ischio or pubic ramus fractures [28], which is consistent with the types of injury observed in the experimental data used in this study. Adding PS and SI Joint Force resulted in a better predictor than the PS force only, but still appeared to be worse than the impactor force.

Leport *et al.* [14] proposed IRCs for PMHS at 45 years old based on the pubic force. The pubic force corresponding to 50% risk was 3.13 kN, which is slightly lower than the 3.62 kN found in this study for the THUMS v4 at the same age, but higher than the associated lower limit of the confidence interval (2.67 kN). In [14], the ratio of the pubic force to the impactor force observed on a series of low energy tests was used to calculate the pubic force for a wider set of tests reported in the literature. The pubic ratios calculated for the THUMS v4 were 26% and 20%, on average, for the impactor configuration and for the mini-sled configuration, respectively. Leport *et al*. found 30% and 22%, but for the mini-sled configuration this ratio varied significantly from test to test. Leport *et al*. used a rigid force sensor at the PS and highlighted that it most likely caused the pubic force to be overestimated to some extent. To summarize, the differences between the THUMS v4 pubic IRC and the PMHS IRC reported in Leport *et al.* could come from discrepancies in the datasets used, an under-prediction of the pubic force in the model or errors inherent to the method used by Leport *et al*. to calculate pubic forces.

Kemper *et al.* in 2008 [29] reported tensile tests performed on pelvic cortical bone samples in which four PMHS were used and the following locations were tested: anterior/posterior ilium, superior pubic ramus and ischium body. Due to the small number of tests, it was not possible to arrive at a statistically significant result, nonetheless it seems that failure strain levels could depend on the location and orientation of the samples. Kemper *et al*. [12][30] also reported strain failure levels for the anterior ribs of 2.4+-0.9% and the axial tibia of 1.8+-0.14%, with larger sample sizes (n=94 and n=20). The MPS IRC with acetabulum showed 50% risk at 2.3% strain for an age of 67 years old, which is comparable to the values reported by Kemper *et al*. One important limitation of the current study arises from not considering regional [29] and directional [29][31] dependency of the failure level and using homogeneous and isotropic local injury criterion. It was not possible in this study to directly correlate the strains measured on the model to those of the PMHS, therefore we cannot conclude if the strains predicted in the model are correct.

Results of Bouquet 1994 simulations stood out for all predictors, indeed the risks predicted for this test series were very low when compared to the injury outcome. The calculated risks for all the tests simulated for this configuration and for the MPS95 with acetabulum predictor are highlighted on Graph 18.

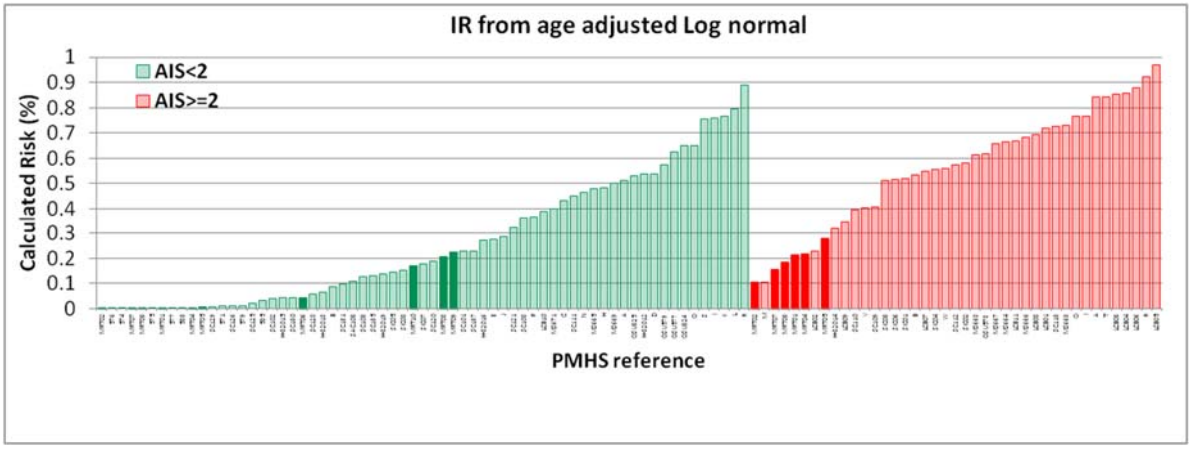

Fig. 18. MPS95 AIS2+ risks for Bouquet 1994.

Six out of nine tests performed at an impact speed of 6.5 m/s sustained AIS2+ injuries, however the maximum risk calculated from the simulations out of these nine tests was 28%. Results were similar for all tested predictors. It seems very unlikely, therefore, that the calculated risks for this test series are representative of the actual risk. It was highlighted in the Results section that the impactor force measured in the simulation for this test series was low in comparison with the corresponding experiments. It could be that the test conditions were not correctly reproduced in the simulations, yet they were rather well documented. Removing these tests in the development of the IRC would shift the IRC slightly, as can be seen in Fig. 19. It should be noted that the IRC obtained excluding the test series is contained in the 95th confidence intervals of the IRC including them, except for the very low MPS values, where excluding them leads to lower risk prediction.

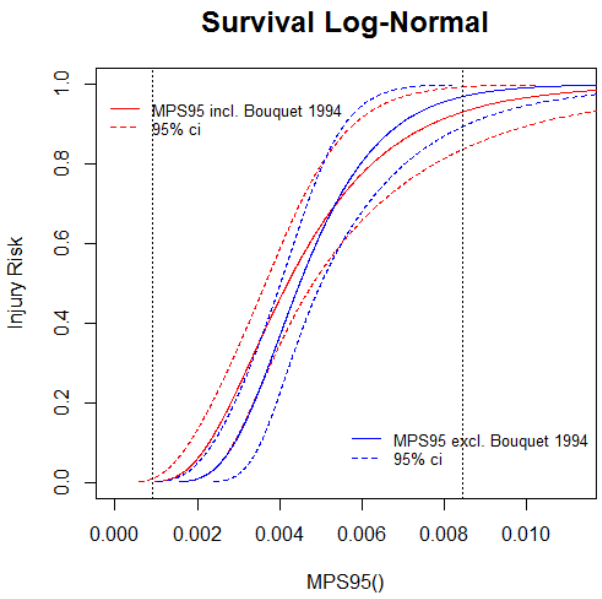

Fig. 19. Comparison of MPS95 IRCs with and without Bouquet 1994.

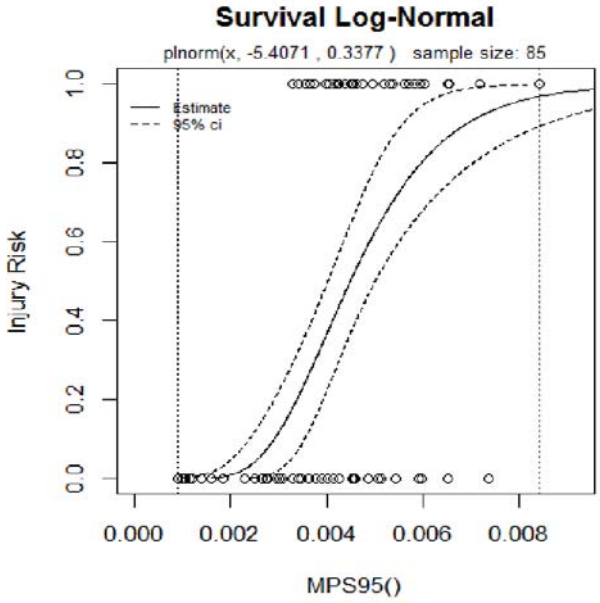

Fig. 20. Log normal IRC for MPS95 without Bouquet 1994.

Results obtained for the Cesari simulations also stand out as they exhibit high risks for several tests that did not result in injuries (see Fig. 21 for the MPS95 with acetabulum). In this test set-up, the impact is local and involves the great trochanter only, the whole load is thus transmitted directly to the acetabulum through the Femur head. In this case, the over-prediction of the strain in the acetabulum generally observed in the THUMS could be amplified, leading to higher risks than expected. When excluding the acetabulum from the predictor, the risks are slightly lower for this test series, but the improvement is not significant.

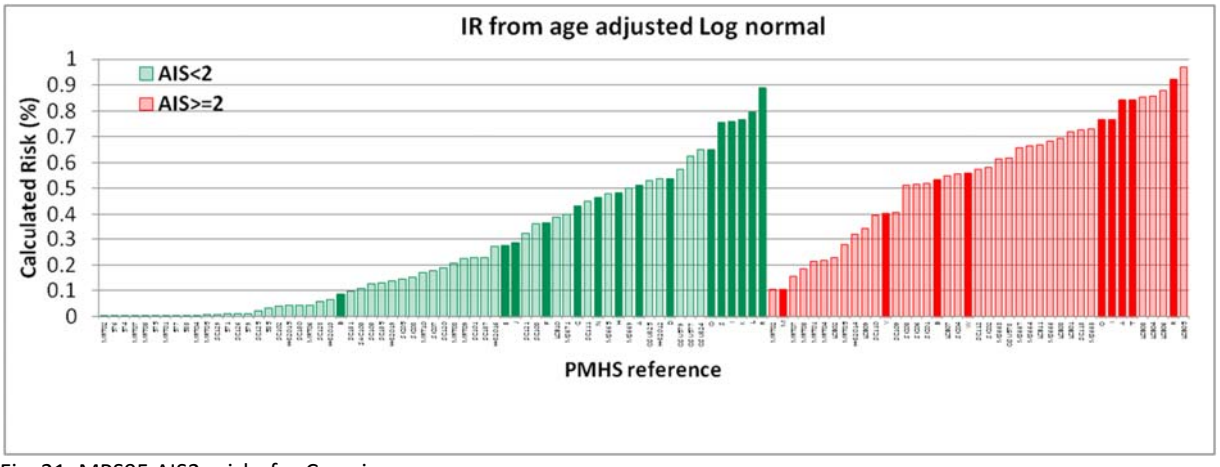

Fig. 21. MPS95 AIS2+ risks for Cesari.

It appears that for a given predictor, the difference between log-logistic, log-normal and Weibull distributions is not significant, as illustrated in Table VIII. The AUC of the ROC curves are lower for the global predictors than the locals, which would indicate a lesser ability to discriminate between the non-injured and injured cases. Quality indexes of the risk curves at 5%, 25% and 50% are all inferior to 0.5, which is classified as good considering the ISO recommendations. Age effect improves the AIC values significantly for most predictors and distributions, Impactor force showing the highest age-related gain.

Despite these similarities between the results observed for the different predictors, only three exhibit an age-adjusted AIC below 124, namely MPS without acetabulum, MPS99 and MPS95 with acetabulum. These three predictors also happen to have AUC values over 0.8 and quality indexes below 0.3 for 5%, 25% and 50% risks of injury. MPS without acetabulum exhibits the lowest AIC values between these three but the highest quality indexes, even if those remain good. MPS is a local predictor that considers only one element and is therefore believed to be sensitive to modeling-related local strain concentrations, which could potentially be detrimental to the robustness of this criteria for other loading configurations, leading us not to recommend its use. MPS99 and MPS95 with acetabulum show very little difference for all evaluation criteria, the difference between AIC with age adjustment not being statistically significant. The parameter study indicated that MPS95 is less sensitive to variations of the setup than MPS99. It would be possible to investigate lower percentiles of the strain distribution, which would most likely lead to even more robust criteria, however fracture is essentially a local phenomenon and we therefore focused on local strain predictors. A tradeoff certainly exists between robustness and injury prediction capability which should be further investigated.

Finally, it was not possible to objectively discriminate between these two injury predictors and, at this stage, it is recommended to use MPS95 and/or MPS99 measured on the cortical elements of the pelvis, including the acetabulum, as pelvic injury criterion for the THUMS v4 AM50. It was decided to keep the Bouquet 1994 test series in the dataset as this leads to the injury prediction being conservative for the lower severity levels, with the influence proving to be limited at higher severities. Injury risk curves are proposed for MPS95 and MPS99 for ages of 45 and 65 years old on Figs 22–25. Injury risk curves could be produced for other ages, but it is not recommended to do it for ages too far from the average age of the PMHS used to develop the IRCs (67 years old) as the confidence intervals would be wider. Quality indexes for MPS95 and MPS99 with acetabulum at 45 years old are summarized in Table V.

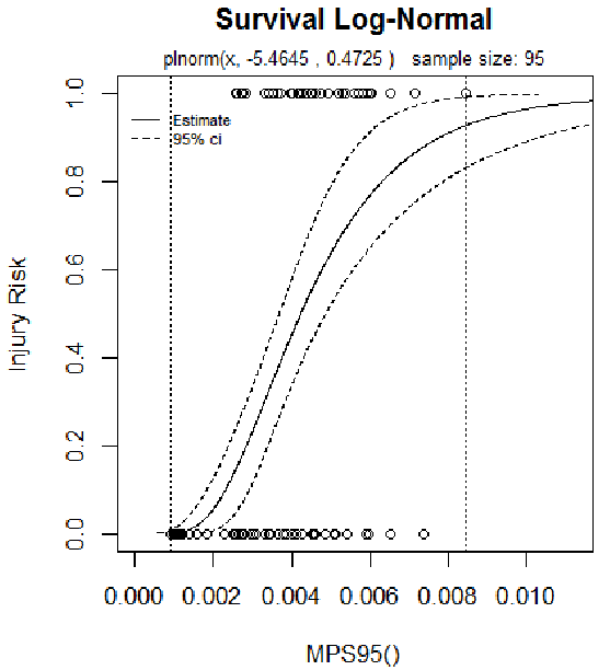

Fig. 22. Log normal IRC for MPS95 with acetabulum at 65YO.

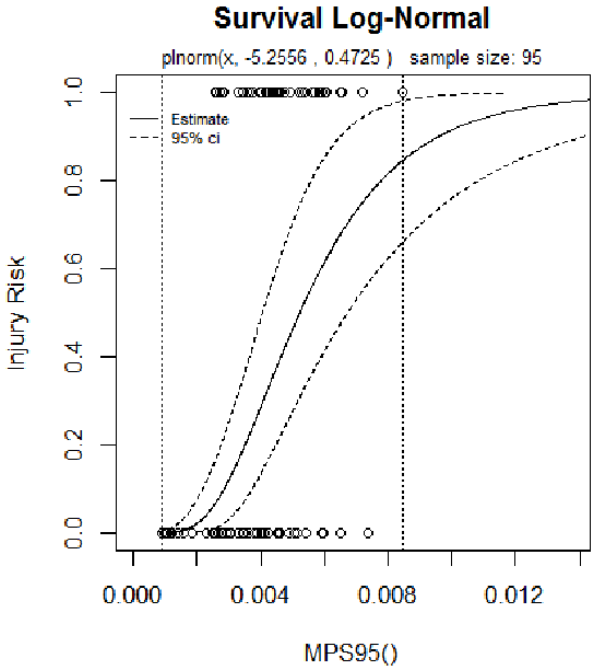

Fig. 23. Log normal IRC for MPS95 with acetabulum at 45YO.

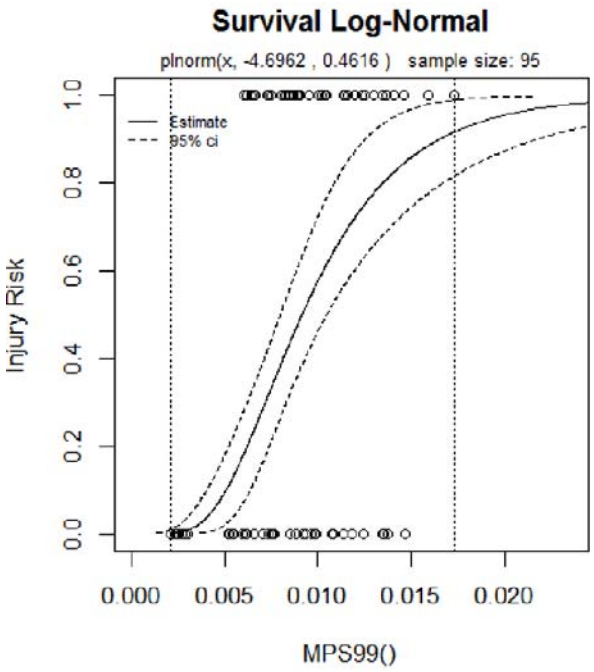

Fig. 24. Log normal IRC for MPS99 with acetabulum at 65YO.

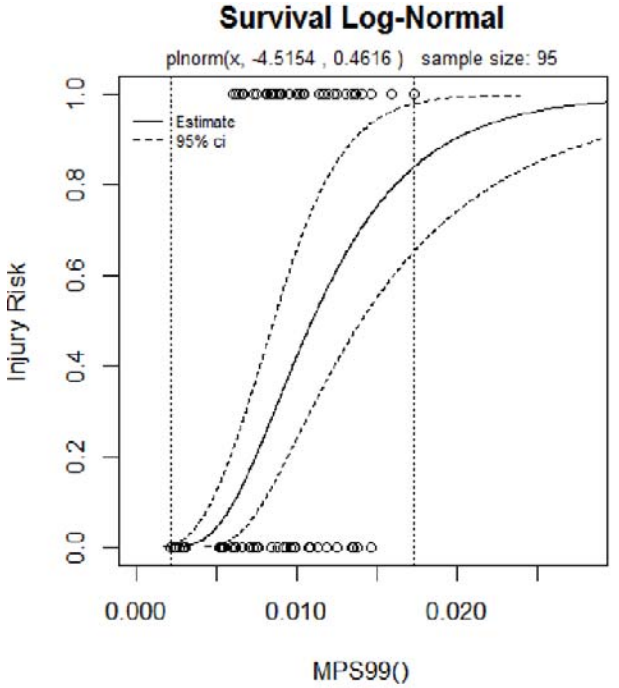

Fig. 25. Log normal IRC for MPS99 with acetabulum at 45YO.

TABLE V
QUALITY INDEXES AT 45 YEARS OLD FOR LOG-NORMAL DISTRIBUTIONS

Predictor	QI at 5% risk	QI at 25% risk	QI at 50% risk
MPS95 without acetabulum	0.25	0.21	0.21
MPS95 with acetabulum	0.25	0.21	0.21

Limitations

Several limitations emerge in this study, the first of which arises from the lack of some important information on the experimental tests. For example, it is likely that the posture of the PMHS varied between the different tests, however one standard position was used for the whole simulations. A parametric study was performed and showed that the sensitivity depends on the predictor. It seems that the THUMS v4 model was not extensively validated for the pelvis region as only one validation test is reported [32]. Nonetheless, impactor forces and pubic forces measured on the model correlated well with experimental results in this study. No correlation could be performed between the strains measured on the model and those of the PMHS tests.

Additionally, only rigid impactors were used and only one test series (SI Joint), comprising nine tests, involved angled impactors. Automotive side impacts involve much more complicated and diverse conditions, which might modify the load path through the pelvis. Including padded as well as additional angled impacts would improve the ability of the IRC to be applicable to more realistic crash conditions. Real accident reconstructions could be used to better assess the injury prediction capabilities.

Impactor dimensions were not scaled, which likely results, for PMHS far from the 50th percentile, in different areas of the body being engaged in the impact in the experiment and the simulation. This could lead to discrepancies in cases where, for example, one engages the iliac wing and the other note. More assumptions linked to the normalizing method originate from geometrical similarity and stiffness equivalence between the different cadavers.

Caution is advised in the use of the IRCs for low risk levels as a large initial step was systematically observed in the non-parametric distribution and the inclusion or exclusion of the Bouquet 1994 test series led to significant modifications in this region. Only AIS2+ injuries were investigated in this study because for some PMHS, it was the only information available. As already mentioned, the use of homogeneous and isotropic criterion for the strain might not be representative of the complexity of the pelvic bone, which potentially has failure limits depending on the location and the orientation. Unfortunately, few data are available to characterize it further.

V. CONCLUSION

PMHS lateral impact tests to the pelvis from the literature were selected and reproduced with the THUMS v4 AM50, allowing the development of IRCs predicting AIS2+ pelvis injuries. Several injury criteria were investigated and the 95th and 99th percentile of the MPS distribution on the pelvis cortical bone are recommended as injury criterion. Injury risk curves developed using a log-normal survival analysis, including age adjustment, are proposed. Further work would be needed to investigate potential modelling improvement of the THUMS v4 at the hip joint as well as the inclusion of more realistic and diverse impact conditions in the database to improve the risk prediction. Deeper analysis on the location of the maximum strains in the simulations and their correlation with observed experimental injuries will be conducted. The poor prediction ability of the pubic symphysis in this study is not well understood, therefore comparisons with an existing WSID FE model and associated IRCs are being completed to investigate this aspect further.

VI. REFERENCES

[1] National Highway Traffic Safety Administration. Traffic safety facts: A compilation of motor vehicle crash data from the Fatality Analysis Reporting System and the General Estimates System. Internet: [http://www-nrd.nhtsa.dot.gov/Cats/listpublications.aspx?Id=E&ShowBy=DocType] [accessed 8 April 2016].

[2] Acierno, S., Kaufman, R., Rivara, F. P., Grossman, D. C., Mock, C. (2004) Vehicle Mismatch: Injury Patterns and Severity. *Accident Analysis & Prevention*, **36**(5): pp.761–72.

[3] Hell, W., Langwieder, K., Sporner, A. Injury patterns compared to injury costs in car to car accidents of belted occupants with major injuries. (1999) *Proceedings of the 43rd Association for the Advancement of Automotive Medicine*, Barcelona, Spain, pp.119–38.

[4] Ryan, E. Hernias related to pelvic fractures. (1971) *Surgery, gynecology and obstetrics.,* **133**(3): pp.440–46.

[5] Stein, D., O´Connor, J. *et al*. (2006) Risk factors associated with pelvic fractures sustained in motor vehicle collisions involving newer vehicles. *J Trauma.* **61**(1): pp.21–30.

[6] Lobdell, T., Kroell, C., Schneider, D., Hering, W., Nahum, A. Impact Response of the Human Thorax, pp. 201–45. *Proceedings of the Symposium from Human Impact Response Measurement and Simulation*, 1973, New York. *Plenum Press*, Germany.

[7] Shigeta, K., Kitagawa, Y., Yasuki, T. Development of next generation human FE model capable of organ injury prediction. *Proceedings of the 21st International Conference on Enhanced Safety vehicles (ESV),* 2009, Stuttgart, Germany.

[8] Thompson, A., Gayzik, F. *et al*. (2012) A paradigm for human body finite element model integration from a set of regional models. *Biomed Sci Instrum,* **48**: pp.423–30.

[9] Beillas, P., Petit, P. *et al*. Specifications of a Software Framework to Position and Personalise Human Body Models. *Proceedings of the IRCOBI Conference*, 2015, Lyon, France, IRC-15-66.

[10] Shi, X., Cao, L. *et al*. (2014) A statistical human rib cage geometry model accounting for variations by age, sex, stature and body mass index. *Journal of Biomechanics,* **47**(10): pp. 2277–85.

[11] Forman, J., Kent, R. *et al*. (2012) Predicting rib fracture risk with whole body finite element models: development and preliminary evaluation of a probabilistic analytical framework. *Ann Adv Automot Med*, **56**: pp.109–24.

[12] Kemper, A. McNally, C. *et al*. (2005) Material properties of human rib cortical bone from dynamic tension coupon testing. *Stapp Car Crash J*, **49**: pp.199–230.

[13] Salzar, R., Genovese, D. *et al*. (2009) Load path distribution within the pelvic structure under lateral loading. *Int J. Crashworthiness,* **14**(1): pp.99–110.

[14] Leport, T., Baudrit, P. *et al*. (2007) Assessment of the pubic force as a pelvic injury criterion in side impact. *Stapp Car Crash J.,* **51**: pp.467–88.

[15] Petitjean, A., Trosseille, X., Praxl, N., Hynd, D., Irwin, A. (2012) Injury risk curves for the WorldSID 50th male dummy. *Stapp Car Crash J.,* **56**: pp.323–47.

[16] Mertz, H. (1984) A Procedure For Normalizing Impact Response Data. *SAE Paper* No. 840884.

[17] Eppinger, R., Marcus, J., Morgan, R. (1984) Development of Dummy and Injury Index for NHTSA's Thoracic Side Impact Protection Research Program. *SAE Paper* No. 840885. Government/Industry Meeting and Exposition, Washington, D.C. *Society of Automotive Engineers*, Warrendale, PA.

[18] ISO/TC 22/SC 12/WG 6 TS18506: Road vehicles — Procedure to construct injury risk curves for the evaluation of road users' protection in crash tests. (2014) *International Standards Organization*. American National Standards Institute, New York.
[19] Cesari, D., Ramet, M,, Clair, P. (1980) Evaluation of pelvic fracture tolerance to side impact. *Stapp Car Crash J.*, **24**: pp. 145–54.
[20] Cesari, D., Ramet, M. (1982) Pelvic tolerance and protection criteria in side impact. *Stapp Car Crash J.*, **26**: pp. 145–54.
[21] Marcus, J., Morgan, R. *et al*. (1983) Human Response to an Injury from Lateral Impact. *Stapp Car Crash J.*, **27**: pp.419–32.
[22] Zhu, J., Cavanaugh, J., King, A. (1993) Pelvic biomechanical response and padding benefits in side impact based on a cadaveric test series. *Stapp Car Crash J.*, **37**: pp.223-33.
[23] Pintar, F., Yoganandan, N. *et al.* (1997) Chestband analysis of human tolerance to side impact. *Stapp Car Crash J.*, **41**: pp.211–41.
[24] Kuppa, S., Eppinger, R. *et al.* (2003) Development of Side Impact Thoracic Injury Criteria and Their Application to the Modified ES-2 Dummy with Rib Extensions (ES-2re). *Stapp Car Crash J.,* **47**: pp.189–210.
[25] Bouquet, R., Ramet, M. Thoracic and pelvis human response to impact. *Proceedings of the 14th International Conference on Enhanced Safety vehicles (ESV)*, 1994, Munich, Gemany.
[26] Bouquet, R., Ramet, M. *et al*. Pelvis Human Response to Lateral Impact. *Proceedings of the 16th International Conference on Enhanced Safety vehicles (ESV),* 1998, Windsor, Ontario, Canada.
[27] Petit, P., Trosseille, X. *et al*. (2015) A Comparison of Sacroiliac and Pubic Rami Fracture Occurrences in Oblique Side Impact Tests on Nine Post Mortem Human Subjects. *Stapp Car Crash J.*, **59**: pp.23–52.
[28] Guillemot, H., Besnault, B. *et al*. (1997) Pelvic injuries in side impact collisions: an accidental analysis and dynamic tests on isolated pelvic bones. *Stapp Car Crash J.*,**41**: pp.91–100.
[29] Kemper, A., McNally, C., Duma, S. (2008) Dynamic tensile material properties of human pelvic cortical bone. *Biomed Sci Instrum.,* **44:** pp.417–18.
[30] Kemper, A., McNally, C*. et al*. (2008) The biomechanics of human ribs: material and structural properties from dynamic tension and bending tests. *Stapp Car Crash J.,* **51**: pp.235–73.
[31] Kemper, A., McNally, C., Kennedy, E., Manoogian, S., Duma, S. The material properties of the human tibia cortical bone in tension and compression: implications for the tibia index. *Proceedings of the 21st International Conference on Enhanced Safety vehicles (ESV)*, 2007, Lyon, France.
[32] THUMS v4.02 documentation. THUMS_AM50_V402_Document_20150527.pdf. *Toyota Motor Corporation.*

Appendix

Details of all simulated test conditions

TABLE VI ALL SIMULATIONS RESULTS

Test serie	Test ref.	Impact speed (m/s)	Impact Force (N)	Pubic Force (N)	PS+SIJ Force (N)	MPS without acet. ()	MPS with acet. ()	MPS99 without acet. ()	MPS99 with acet. ()	MPS95 without acet ()	MPS95 with acet. ()
Cesari	A3	9.3	10246	2512	4678	0.0216	0.0249	0.0069	0.0098	0.0041	0.0041
Cesari	A4	12.7	15625	3519	6160	0.0374	0.0393	0.0117	0.0146	0.0065	0.0065
Cesari	B1	6.1	5120	1553	3265	0.0066	0.0112	0.0024	0.0053	0.0018	0.0018
Cesari	B2	8.7	9202	2317	4390	0.0186	0.0221	0.0060	0.0089	0.0037	0.0037
Cesari	C2	8.8	9494	2371	4470	0.0194	0.0229	0.0063	0.0092	0.0038	0.0038
Cesari	D2	10.0	11251	2700	4955	0.0246	0.0276	0.0078	0.0107	0.0046	0.0046
Cesari	E1	7.7	7747	2044	3989	0.0143	0.0182	0.0047	0.0076	0.0030	0.0030
Cesari	F1	9.0	9703	2410	4528	0.0200	0.0235	0.0065	0.0094	0.0039	0.0039
Cesari	H3	9.2	10026	2471	4617	0.0210	0.0243	0.0067	0.0096	0.0040	0.0040
Cesari	I4	12.0	14413	3292	5826	0.0338	0.0360	0.0106	0.0135	0.0060	0.0060
Cesari	I5	12.1	14549	3317	5864	0.0342	0.0364	0.0108	0.0137	0.0060	0.0060
Cesari	J1	7.6	7620	2021	3954	0.0140	0.0179	0.0046	0.0075	0.0029	0.0029
Cesari	K3	11.2	13202	3065	5492	0.0303	0.0328	0.0096	0.0125	0.0054	0.0054
Cesari	L4	11.9	14287	3268	5792	0.0335	0.0357	0.0105	0.0134	0.0059	0.0059
Cesari	M3	6.7	6118	1740	3540	0.0096	0.0139	0.0033	0.0062	0.0023	0.0023
Cesari	N6	10.0	11320	2713	4974	0.0248	0.0278	0.0079	0.0108	0.0046	0.0046
Cesari	O5	10.4	11924	2826	5140	0.0265	0.0294	0.0084	0.0113	0.0049	0.0049
Cesari	O6	11.6	13824	3182	5664	0.0321	0.0345	0.0101	0.0130	0.0057	0.0057
Cesari	R4	12.8	15656	3525	6169	0.0375	0.0394	0.0118	0.0147	0.0065	0.0065
Cesari	R5	13.7	17095	3794	6566	0.0417	0.0432	0.0130	0.0159	0.0072	0.0072
Cesari	S2	10.8	12520	2938	5305	0.0283	0.0310	0.0090	0.0119	0.0051	0.0051
Cesari	T2	11.9	14328	3276	5803	0.0336	0.0358	0.0106	0.0135	0.0059	0.0059
Cesari	V2	9.1	9910	2449	4585	0.0207	0.0240	0.0066	0.0095	0.0040	0.0040
Cesari	W2	8.8	9366	2347	4435	0.0191	0.0226	0.0062	0.0091	0.0037	0.0037
Marcus	H-82012	11.3	30394	4104	8605	0.0443	0.0138	0.0106	0.0138	0.0073	0.0074
Marcus	H-82014	9.1	21960	3345	6813	0.0300	0.0104	0.0075	0.0104	0.0053	0.0054
Marcus	H-82015	6.5	12259	2472	4753	0.0137	0.0066	0.0039	0.0066	0.0030	0.0031
Marcus	H-82016	8.8	20694	3231	6545	0.0279	0.0099	0.0071	0.0099	0.0050	0.0051
Marcus	H-82018	6.5	12259	2472	4753	0.0137	0.0066	0.0039	0.0066	0.0030	0.0031
Marcus	H-82019	6.5	12259	2472	4753	0.0137	0.0066	0.0039	0.0066	0.0030	0.0031
Bouquet	LCB01	13.2	21058	2989	6560	0.0257	0.0268	0.0084	0.0125	0.0041	0.0056
Bouquet	LCB02	9.9	14075	2254	4907	0.0195	0.0207	0.0053	0.0084	0.0031	0.0034
Bouquet	LCB03	14.2	25753	3606	7729	0.0335	0.0347	0.0101	0.0136	0.0057	0.0060
Bouquet	LCB04	12.7	19653	2854	6264	0.0238	0.0250	0.0078	0.0119	0.0038	0.0053
Bouquet	LCB05	17.2	33124	4149	9099	0.0417	0.0424	0.0136	0.0173	0.0065	0.0084
Bouquet	LCB06	14.5	24987	3367	7387	0.0309	0.0319	0.0101	0.0141	0.0049	0.0065
Bouquet	LCB07	11.2	17679	2672	5778	0.0238	0.0250	0.0068	0.0100	0.0039	0.0042
Bouquet	LCB08	13.1	22855	3271	7029	0.0300	0.0312	0.0089	0.0123	0.0051	0.0054
Bouquet	LCB09	10.1	14681	2325	5054	0.0202	0.0214	0.0056	0.0087	0.0032	0.0035
Bouquet	LCB10	10.1	11836	2102	4619	0.0134	0.0148	0.0044	0.0088	0.0023	0.0035
Bouquet	LCB11	12.2	18145	2709	5947	0.0218	0.0230	0.0072	0.0113	0.0035	0.0049
Leport	PCH1740	4.0	5307	1036	1875	0.0048	0.0083	0.0017	0.0028	0.0008	0.0012
Leport	PCH1748	3.3	3807	767	1403	0.0033	0.0061	0.0013	0.0021	0.0006	0.0009
Leport	PCH1749	3.6	4459	884	1608	0.0040	0.0070	0.0015	0.0024	0.0007	0.0010
Leport	PCH1750	3.3	3807	767	1403	0.0033	0.0061	0.0013	0.0021	0.0006	0.0009
Leport	PCH1751	3.6	4504	892	1622	0.0040	0.0071	0.0015	0.0024	0.0007	0.0010
Leport	PCH1770	3.5	4264	849	1547	0.0037	0.0067	0.0014	0.0023	0.0006	0.0010
Leport	IMP562	4.0	3023	794	1602	0.0072	0.0072	0.0018	0.0028	0.0009	0.0011
Leport	IMP564	4.1	3555	930	1885	0.0086	0.0086	0.0018	0.0030	0.0011	0.0014
Pintar	OSU324	8.9	14188	2927	6524	0.0253	0.0261	0.0070	0.0085	0.0044	0.0045
Pintar	OSU325	8.9	14188	2927	6524	0.0253	0.0261	0.0070	0.0085	0.0044	0.0045
Pintar	OSU577	8.9	14188	2927	6524	0.0253	0.0261	0.0070	0.0085	0.0044	0.0045

Pintar	OSU578	8.9	14188	2927	6524	0.0253	0.0261	0.0070	0.0085	0.0044	0.0045
Pintar	OSU579	8.9	14188	2927	6524	0.0253	0.0261	0.0070	0.0085	0.0044	0.0045
Kuppa	SAC102	6.7	8458	2148	4563	0.0108	0.0149	0.0041	0.0054	0.0027	0.0028
Kuppa	SC101	6.7	8458	2148	4563	0.0108	0.0149	0.0041	0.0054	0.0027	0.0028
Kuppa	SC102	6.7	8458	2148	4563	0.0108	0.0149	0.0041	0.0054	0.0027	0.0028
Kuppa	SC103	6.7	8458	2148	4563	0.0108	0.0149	0.0041	0.0054	0.0027	0.0028
Kuppa	SC108	8.9	14188	2927	6524	0.0253	0.0261	0.0070	0.0085	0.0044	0.0045
Kuppa	SC109	8.9	14188	2927	6524	0.0253	0.0261	0.0070	0.0085	0.0044	0.0045
Kuppa	SC110	6.7	13287	2480	4793	0.0145	0.0178	0.0048	0.0073	0.0029	0.0033
Kuppa	SC111	6.7	13287	2480	4793	0.0145	0.0178	0.0048	0.0073	0.0029	0.0033
Kuppa	SC112	7.6	16320	2838	5490	0.0190	0.0197	0.0059	0.0090	0.0037	0.0040
Kuppa	SC113	8.9	20481	3308	6429	0.0257	0.0257	0.0077	0.0114	0.0047	0.0052
Kuppa	SC120	6.7	8458	2148	4563	0.0108	0.0149	0.0041	0.0054	0.0027	0.0028
Kuppa	SC121	6.7	8458	2148	4563	0.0108	0.0149	0.0041	0.0054	0.0027	0.0028
Kuppa	SC125	6.7	3284	1153	3122	0.0054	0.0079	0.0023	0.0030	0.0014	0.0016
Kuppa	SC126	6.7	3284	1153	3122	0.0054	0.0079	0.0023	0.0030	0.0014	0.0016
Kuppa	SC128	6.7	8458	2148	4563	0.0108	0.0195	0.0036	0.0055	0.0027	0.0025
Kuppa	SC129	6.7	3284	1153	3122	0.0054	0.0079	0.0023	0.0030	0.0014	0.0016
Kuppa	SC130	6.7	8458	2148	4563	0.0108	0.0195	0.0036	0.0055	0.0027	0.0025
Kuppa	SC131	6.7	8458	2148	4563	0.0108	0.0149	0.0041	0.0054	0.0027	0.0028
Kuppa	SC135	6.7	8458	2148	4563	0.0108	0.0149	0.0041	0.0054	0.0027	0.0028
Kuppa	SC137	6.7	8458	2148	4563	0.0108	0.0149	0.0041	0.0054	0.0027	0.0028
Zhu	SIC01	8.9	17151	3149	5330	0.0305	0.0305	0.0069	0.0102	0.0042	0.0046
Zhu	SIC02	9.1	17716	3210	5398	0.0318	0.0318	0.0071	0.0103	0.0043	0.0048
Zhu	SIC03	10.5	21367	3697	6162	0.0467	0.0467	0.0089	0.0116	0.0054	0.0058
Zhu	SIC04	9.1	16670	3032	6003	0.0277	0.0277	0.0068	0.0085	0.0040	0.0044
Zhu	SIC05	9.0	10489	2197	4315	0.0130	0.0154	0.0039	0.0053	0.0025	0.0027
Zhu	SIC06	6.7	16366	2991	5941	0.0267	0.0267	0.0066	0.0083	0.0039	0.0043
Zhu	SIC07	6.7	10489	2197	4315	0.0130	0.0154	0.0039	0.0053	0.0025	0.0027
Zhu	SIC08	6.6	10330	2146	4226	0.0123	0.0150	0.0038	0.0051	0.0024	0.0027
Bouquet	MRB01	3.4	3256	791	1577	0.0034	0.0068	0.0012	0.0023	0.0009	0.0010
Bouquet	MRB02	6.6	7734	1632	3311	0.0110	0.0160	0.0034	0.0062	0.0022	0.0026
Bouquet	MRB03	3.4	3211	783	1559	0.0033	0.0067	0.0012	0.0023	0.0009	0.0010
Bouquet	MRB04	6.5	7579	1603	3251	0.0107	0.0157	0.0034	0.0060	0.0021	0.0026
Bouquet	MRB05	3.5	3340	807	1609	0.0035	0.0070	0.0013	0.0024	0.0009	0.0011
Bouquet	MRB06	7.0	8189	1717	3488	0.0118	0.0170	0.0037	0.0065	0.0023	0.0028
Bouquet	MRB07	3.7	3690	873	1745	0.0041	0.0077	0.0014	0.0027	0.0010	0.0012
Bouquet	MRB08	7.1	8346	1747	3548	0.0121	0.0173	0.0037	0.0067	0.0023	0.0028
Bouquet	MRB09	3.6	3435	825	1646	0.0037	0.0071	0.0013	0.0025	0.0009	0.0011
Bouquet	MRB10	7.1	8330	1744	3542	0.0120	0.0172	0.0037	0.0067	0.0023	0.0028
Bouquet	MRB12	6.4	7481	1585	3213	0.0106	0.0155	0.0033	0.0059	0.0021	0.0025
Bouquet	MRB13	3.6	3412	821	1637	0.0036	0.0071	0.0013	0.0025	0.0009	0.0011
Bouquet	MRB14	6.8	8017	1685	3421	0.0115	0.0166	0.0036	0.0064	0.0022	0.0027
Bouquet	MRB16	7.0	8229	1725	3503	0.0119	0.0170	0.0037	0.0066	0.0023	0.0028
Bouquet	MRB18	6.5	7499	1588	3220	0.0106	0.0155	0.0033	0.0060	0.0021	0.0025
Bouquet	MRB20	6.6	7666	1619	3285	0.0109	0.0159	0.0034	0.0061	0.0021	0.0026
SI_Joint	PCH2123	8.1	16183	1826	5653	0.0249	0.0249	0.0081	0.0080	0.0043	0.0045
SI_Joint	PCH2124	8.2	16599	1854	5775	0.0257	0.0257	0.0082	0.0082	0.0044	0.0046
SI_Joint	PCH2125	7.8	15317	1711	5427	0.0224	0.0224	0.0076	0.0076	0.0041	0.0043
SI_Joint	PCH2128	5.5	6065	1009	3832	0.0252	0.0252	0.0085	0.0081	0.0045	0.0045
SI_Joint	PCH2129	5.4	5903	958	3719	0.0252	0.0231	0.0085	0.0075	0.0045	0.0042
SI_Joint	PCH2130	5.4	5678	938	3639	0.0220	0.0220	0.0078	0.0073	0.0042	0.0042
SI_Joint	PCH2132	7.4	15692	2007	5558	0.0144	0.0154	0.0053	0.0076	0.0029	0.0036
SI_Joint	PCH2134	7.3	14634	1889	5257	0.0134	0.0148	0.0049	0.0070	0.0027	0.0034

IRCs including Bouquet 1994

TABLE VII BEST DISTRIBUTION FOR MPS WITHOUT ACET., MPS95 AND MPS99 WITH ACET.

Predictor	Distribution	Mean	Standard deviation	Age adjustment coefficient
MPS 95 with acet.	Log-normal	-5.475	0.4725	-0.0104
MPS 99 with acet.	Log-normal	-4.705	0.4616	-0.0090
MPS without acet.	Log-normal	-3.838	0.6130	-0.0145

IRCs evaluation including Bouquet 1994

TABLE VIII EVALUATION OF ALL DISTRIBUTIONS FOR EACH PREDICTOR INCLUDING BOUQUET 1994.

Criteria	Distribution	AIC		QI at 5% risk	QI at 25% risk	QI at 50% risk
		Without age adjustment	With age adjustment			
Impactor Force	Log logistic	135.3	126.9	0.29	0.16	0.15
	Log Normal	135.2	125.9	0.25	0.16	0.15
	Weibull	136.1	125.5	0.32	0.17	0.13
Pubic Force	Log logistic	152.5	144.7	0.32	0.17	0.15
	Log Normal	152.7	144.0	0.27	0.16	0.15
	Weibull	150.4	142.9	0.34	0.17	0.13
PS+SI	Log logistic	143.7	136.6	0.26	0.14	0.12
	Log Normal	143.2	135.9	0.23	0.13	0.12
	Weibull	143.8	135.9	0.29	0.14	0.10
MPS without acet.	Log logistic	126.4	122.2	0.33	0.20	0.17
	Log Normal	125.4	121.2	0.30	0.18	0.16
	Weibull	126.7	121.6	0.38	0.21	0.15
MPS with acet.	Log logistic	125.1	125.9	0.29	0.16	0.14
	Log Normal	123.9	125.4	0.26	0.16	0.14
	Weibull	125.0	125.7	0.32	0.18	0.13
MPS99 without acet.	Log logistic	129.9	128.2	0.35	0.20	0.16
	Log Normal	128.8	130.0	0.29	0.18	0.17
	Weibull	129.4	127.8	0.40	0.22	0.14
MPS 99 with acet.	Log logistic	127.2	124.9	0.28	0.15	0.13
	Log Normal	125.9	123.5	0.24	0.14	0.12
	Weibull	127.7	125.6	0.32	0.16	0.13
MPS 95 without acet.	Log logistic	136.0	131.5	0.29	0.19	0.15
	Log Normal	134.9	130.3	0.27	0.19	0.18
	Weibull	136.3	131.3	0.33	0.21	0.14
MPS 95 with acet.	Log logistic	127.2	123.8	0.28	0.16	0.12
	Log Normal	126.3	122.6	0.26	0.13	0.12
	Weibull	127.7	123.5	0.31	0.16	0.11